General Purpose Bidirectional Optical Backplane: High-performance Bus for Multiprocessor Systems

Chunhe Zhao, Tchang-hun OH, and Ray T. Chen

Microelectronics Research Center
Department of Electrical and Computer Engineering
University of Texas, Austin, Texas 78712-1084

Abstract

We report the first bidirectional optical backplane bus for a high performance multiprocessor system operating at wavelengths of 632.8 nm and 1300 nm. The optical backplane employs an array of multiplexed holograms, in conjunction with a waveguiding plate within which cascaded fanouts are generated. Data transfer rate of 1.2 Gbit/sec at 1300 nm is demonstrated with a single bus line for a system composed of nine processor /memory boards. To provide a reliable system, packaging-related issues, such as the detector size and misalignment effects are addressed. Theoretical treatment to minimize fluctuations among the received power at each processor /memory board is further presented and an optimum design rule is provided. The backplane demonstrated here is for general-purpose. It can support standard multiprocessor buses such as Futurebus+, Multibus II, etc. It also can function as a backplane bus in existing computing systems and significantly reduce the bottlenecks that accompany electrical interconnects.

1. Introduction

Over the past decade, the demand for more computing power has increased to such an extent that no single processor can provide the solutions in many applications. As a result, various efforts were made to build multiprocessor systems. Although there have existed different kinds of multiprocessors systems, those based on electrical backplane buses have been prevailing in the commercial market. However, as the signal speed increases along the backplane, the transmission line effects become dominant, and the performance becomes limited by backplane physics[1]. Although advanced buses like Futurebus+[2] guarantees an incident wave switching, other inherent problems of electrical backplane degrade the performance significantly[3]. As new faster processors arise, the existing backplane buses are subject to saturate, thus can not supply the bandwidth required for high performance multiprocessor systems.

In an effort to increase the interconnection capacity, optics has been considered as an alternative for a long time[4]. Nonetheless, the burden of electrical-to-optical and optical-to-electrical conversions has prevented optics from growing as a viable solution. Recent development of efficient optoelectronic devices, especially in forms of arrays, has stimulated the research seeking for feasible optical solutions. In spite of these efforts, no general optical backplane compatible with existing electrical buses has been announced.

In this paper we report, for the first time, a bi-directional optical backplane bus. Unlike the previous optical backplanes aimed at special purpose computers[5], the backplane reported herein is for general purpose, thus is compatible with standard multiprocessor backplane buses such as Futurebus+, Multibus II[6], etc., as well as any existing backplane bus. The architecture of the bidirectional optical backplane is explained in Section 2. System demonstration containing nine processor/memory boards is described in Section 3. Data rate of 1.2 Gbit/sec for a single bus line is illustrated at 1.3μm wavelength. The theoretical analysis on reliability-related issues is reported in Section 4. The optimization of energy distribution among the nine surface-normal fan-outs is also presented in Section 5. Other system related issues such as packaging and crosstalk are further discussed in Section 6. Finally, the concluding remarks are summarized in Section 7.

2. Bidirectional optical backplane architecture

Fig. 1 shows the schematic of the bi-directional optical backplane in a multiprocessor system with nine processor/memory boards. The backplane bus must provide a path for bidirectional signal flow among the processor/memory boards. To meet this goal, we employ multiplexed holograms in conjunction with a waveguiding plate. Each electrical transceiver at the processor/memory boards drives the corresponding laser diode. The light from the laser is bi-directionally coupled through a multiplexed hologram into the substrate, which acts as a waveguiding plate. The surface-normal fan-outs are provided by an array of holograms located between the backplane and the processor/memory boards. The photodiode associated with each signal line detects light coming from either directions in the waveguiding plate as shown in Fig. 1 (see next page).

IEEE, Proceedings of MPPOI'95

0-8186-7101-7/95 $4.00 © 1995 IEEE

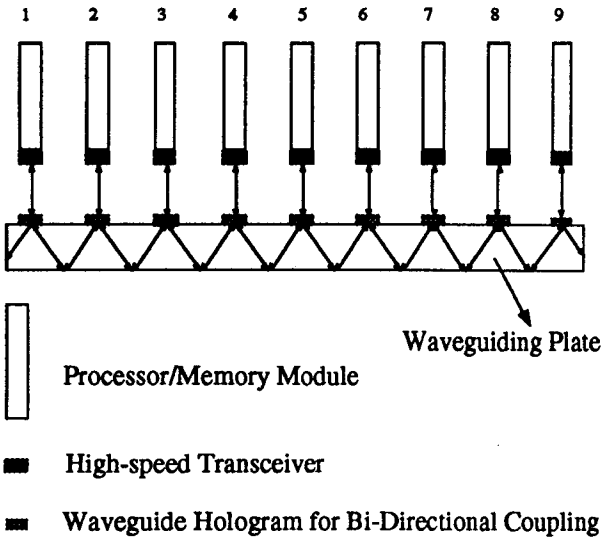

Figure 1. Optical bidirectional backplane bus in a multiprocessor system with nine processor/memory boards

The signal is coupled into the backplane through a hologram acting as an input coupler, which is designed to provide a total-internal-reflected (TIR) beam within the waveguiding plate. An array of multiplexed holograms are recorded along each signal path, as shown in Fig. 1. The actual fabrication process and experimental results are explained in the following section.

A schematic illustrating the diffraction mechanisms associated with the multiplexed holograms is given in Fig. 2. In Fig. 2(a) $\vec{K}_1$ and $\vec{K}_2$ are the grating vectors corresponding to the two gratings recorded inside the polymer film. A normally incident light with a wave vector $\vec{k}$ is phase-matched with both gratings, which have the same Bragg angle. As a result, two diffracted beams with wavevectors $\vec{k}_1'$ and $\vec{k}_2'$ will be generated by the hologram and converted into substrate-guided waves in two opposite directions as shown in Fig. 2(b). During the subsequent transmission processes, whenever the substrate-guided beam hits the multiplexed hologram with the Bragg angle, a part of it is diffracted surface-normally out of the backplane, and detected by the photodiode, while the light with the wavevector $\vec{k}'$ will provide power to the subsequent boards[7]. The optimization of the diffraction efficiencies associated with this process is presented in section 5.

Each multiplexed hologram acts as an input coupler to split a surface normal laser beam of TEM_{00} mode into two substrate-guided beams with a pre-designed bouncing angle of 45°. The same hologram couples a substrate-guided beam into a surface-normal fan-out beam with a specific coupling efficiency. For example, the multiplexed hologram at board 5 (Fig. 1), couples the optical signal from itself to boards 4, 3, 2 and 1 through one grating and to boards 6, 7, 8 and 9 through the other grating. These two gratings are physically multiplexed on top of the waveguiding plate. The same hologram will couple signals generated from boards 4, 3, 2 and 1 to board 5 through the first grating and from boards 6, 7, 8 and 9 to board 5 through the second grating. The function of the bidirectional optical backplane is well understood by its application in a transceiver system. By employing the bidirectional optical bus reported in this paper, each board can send and receive information to and from every other board in the system. Note that the mechanism of cascaded fan-out is employed in all kinds of communications. The control and data signals are broadcast to all boards connected to the backplane.

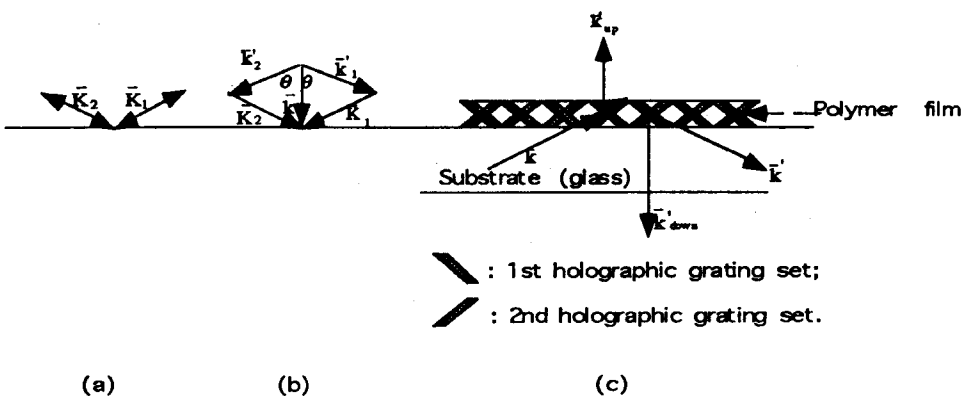

Figure 2. Diffraction mechanism of the multiplexed hologram (a) Two grating vectors recorded (b) Diffraction geometry of the gratings (c) Light transmission, diffraction and reflection inside the bidirectional optical backplane.

3. Experimental results

The physical layer of the optical backplane is a thin waveguige substrate with a set of multiplexed holograms integrated on its surface. The substrate serves as a light-guiding medium. Dichromated gelatin (DCG) is spin-coated on the surface of the substrate. DCG is used as a recording material because of its capability of large refractive index modulation, high resolution, and low absorption and scattering[8]. The recording wavelength for the hologram is 488 nm. The fabrication process[9] is optimized to provide two reconstruction wavelengths at 632.8 nm and 1300 nm.

The recording process is done for one grating first, and after rotating the recording plate by 180° from the previous position, the same process is repeated for the other grating. Two photographs of the bi-directional bus operating at the wavelengths of 632.8 nm and 1300 nm are shown in Figs. 3(a) and 3(b). They show the data transfer from one board to the other 8 boards(1-to-8 transfer). The hologram for the first board is used as an input coupler. The dots in the picture are the far field patterns (without an imaging lens) taken in the surface-normal direction, when the receiving boards are removed to observe far field image. The input beam from board 1 is blocked and therefore not seen in Fig. 3.

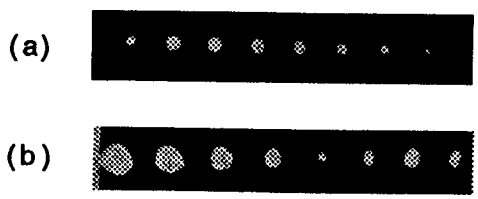

Figure 3. Photograph of the 1-to-8 data transfer (a) operating at 632.8 nm (b) operating at 1300 nm.

In our experiment, the separation between boards is smaller than the electrical standard, which is 3 cm[2]. The separation can be adjusted by using a thicker waveguiding plate or enforcing more reflections inside the waveguiding plate.

The dots in Fig. 3 represent the input lights going to the detectors located on each board. Azimuthal symmetry of the profile is maintained[10], which makes the coupling from the laser to the backplane and then from the backplane to the detector significantly easy. Unlike the conventional guided wave devices where a sizable portion of the surface area is needed to provide the optical signal routing, the substrate-guided-wave-based inter-board interconnect does not require any surface area for this purpose.

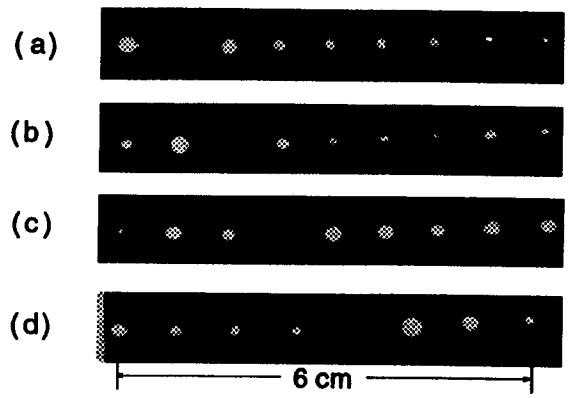

Figure 4. Photographs with (a) the second, (b) the third, (c) the fourth, (d) the fifth boards sending optical signal to the other boards through the bidirectional optical backplane.

Diffraction Efficiency (AU)

Output \ Input	1	2	3	4	5	6	7	8	9
1	0	0.92	0.40	0.16	0.15	0.11	0.07	0.09	0.02
2	0.92	0	0.92	0.40	0.16	0.15	0.11	0.07	0.09
3	0.40	0.92	0	0.92	0.40	0.16	0.15	0.11	0.07
4	0.16	0.40	0.92	0	0.92	0.40	0.16	0.15	0.11
5	0.15	0.16	0.40	0.92	0	0.92	0.40	0.16	0.15
6	0.11	0.15	0.16	0.40	0.92	0	0.92	0.40	0.16
7	0.07	0.11	0.15	0.16	0.40	0.92	0	0.92	0.40
8	0.09	0.07	0.11	0.15	0.16	0.40	0.92	0	0.92
9	0.02	0.09	0.07	0.11	0.15	0.16	0.40	0.92	0

Table 1. Measured fan-out distribution of all the possible input/output combinations of the 1-to-8 bidirectional bus.

The main advantage of our optical backplane stems from its ability to provide the cascaded fan-outs with a signal flow in both directions. This concept is well illustrated in Fig. 4, which shows a set of photographs taken from the bidirectional backplane in the surface-normal direction. Each picture corresponds to a different case where one board is transmitting its signal to the other eight boards. Table 1 shows the measured diffraction efficiencies for all the possible input/output combinations. Note that the experiments are carried out with one hologram as an input coupler and all the other holograms as output couplers. The bi-directionality is demonstrated by the fact that the same multiplexed hologram can be used as both the input

and the output couplers. The input beams are not shown in Fig. 4.

A square wave input can illustrate the performance of the optical backplane in the digital domain. One period of a square wave can accommodate two data bits in non-return-to-zero (NRZ) format. Fig. 5 is a photograph of the output signal received through the backplane when a square wave of 600 MHz or a 1.2 GBit/sec signal is fed to the transmitter. The input is a differential ECL signal and is obtained from a high speed pulse generator. A high speed sampling head is used in conjunction with an oscilloscope to display the output.

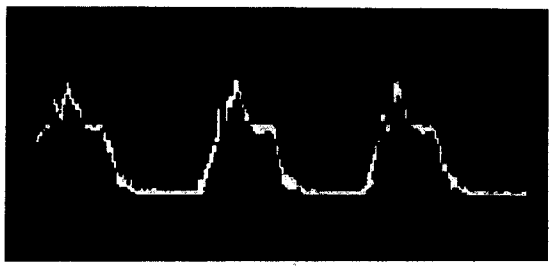

Figure 5. Receiver output from the transceiver system incorporating the bidirectional optical backplane bus for a 1.2 Gbit/sec input signal.

4. Theoretical limits of the system

To enhance the reliability of the optical backplane, theoretical limits are analyzed in various aspects. In an actual system, several factors may influence the performance. In this section we examine the effects of wavelength shift of the laser, transmitter misalignment, and index mismatch between the hologram and the waveguiding plate.

The wavelength of a laser diode is affected by several factors[11]. The wavelength variation ($\delta\lambda$) of the laser has the similar effect as the incident angular perturbation ($\delta\theta$) caused by the transmitter misalignment to the hologram. The relationship between these two effects are given by [12]:

$$\frac{\delta\theta}{\delta\lambda} = \frac{K}{4\pi n \sin(\phi - \theta)} \qquad (1)$$

where λ is the free space wavelength, θ is the incident angle to the hologram, ϕ is the grating slant angle, n is the refractive index of emulsion, and K is the magnitude of the grating vector. In our experiment, $n = 1.5$, $\phi = 22.5^{\circ}$ and $\theta = 0^{\circ}$. The schematic showing these parameters is illustrated in Fig. 6.

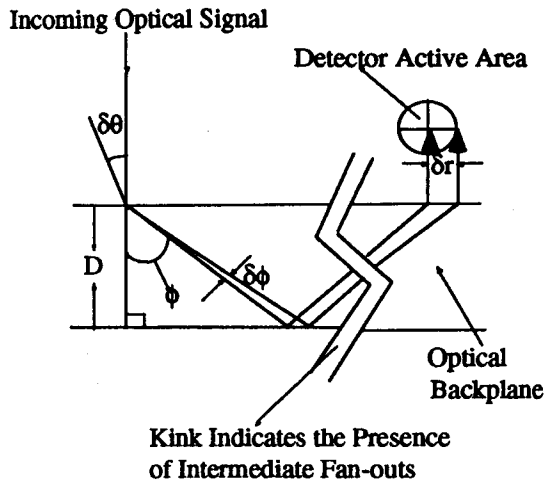

Figure 6. Related parameters for the optical backplane.

The change in diffracted intensity due to the misalignment of the incident light is measured. In our experiment, the maximum angular perturbation, $\delta\theta$, as shown in Fig. 6, is defined as the angular coverage for 1 dB off the peak diffraction intensity. This definition, rather than the 3 dB point, is selected to provide a more reliable power budget for the system. Fig. 7 shows the theoretical and experimental plots quantifying the normalized diffraction intensity (efficiency) as a function of the angular misalignment. The parameters used for the plots are also shown in Fig. 7. For the theoretical case,

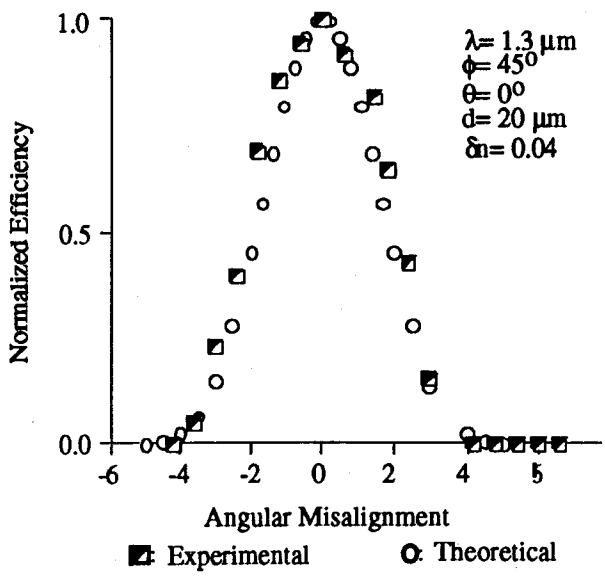

Figure 7. Experimental and theoretical plots showing the relationship between angular misalignment and normalized intensity (efficiency) at 1300 nm.

the overall efficiency is the product of the efficiencies of the input and the output couplers. It results in a close resemblance to the experimental data, which was obtained by measuring the light diffracted by the input and the output couplers. Fig. 7 shows that the 90% diffraction efficiency is obtained with the angular deviation of $\pm 1^{\circ}$, which is the maximum allowable angular misalignment.

Based on (1), the maximum allowable wavelength shift, $\delta\lambda$, of the laser can be determined. The frequency shift, $\delta\nu$, corresponding to $\delta\lambda$ can be calculated according to the following first order approximation:

$$\delta\nu = \frac{c}{\lambda^2}\delta\lambda \tag{2}$$

For example, the wavelength coverage associated with the angular fluctuation of 0.5° is 42 nm, which is equivalent to 7.5 THz of base bandwidth.

The input angular misalignment, $\delta\theta$, will cause a shift in the diffraction angle, $\delta\phi$, in the following way:

$$\delta\phi = -\frac{\cos\theta}{n\cos\phi}\delta\theta \tag{3}$$

where n is the refractive index and ϕ is the desired diffraction angle inside the waveguiding plate. The change in the diffraction angle induced by the wavelength shift of the laser can be calculated by (1) and (3).

The diffracted beam from the output coupler is designed to strike the center of the detector. However, due to the angular shift, it moves along the radius of the detector either as the input angle θ or as the wavelength changes. The maximum lateral shift of the diffracted beam is also limited by size of the detector active area, which has a radius of $100\mu m$ in our experiment. To ensure the reliable operation, we limit the maximum lateral shift by the radius of the detector. The lateral deviation, δL, caused by the change of diffraction angle, $\delta\phi$, is determined by

$$\delta L = 2DN\left[\tan\phi - \tan(\phi \pm \delta\phi)\right] \tag{4}$$

where the substrate thickness, $D = 3mm$, designed diffraction angle, $\phi = 45^{\circ}$, and N indicated the number of bounces experienced by the light inside the waveguiding plate before it reaches the target detector. If we limit the lateral shift, δL, by the radius of the detector, based on (4), (3), and (1), and for communication between the two outermost boards, the wavelength shift should be maintained within 5 nm with no additional angular misalignment. The frequency shift associated with this bandwidth is 0.89 THz.

Up to this point, it has been assumed that the refractive index of the hologram and that of the waveguiding plate are the same. However, as the average refractive index of the DCG hologram is influenced by several effects[13], there may have a difference between the two indices. Since the propagating angle inside the waveguiding plate is affected by both indices, care must be taken to control the refractive index of the hologram precisely.

5. Optimization of fan-out intensities

As far as the power budget is concerned, the performance of the optical backplane is limited by the output channel with the minimum power. For the bidirectional optical bus we report in this paper, the power of the output channels is determined by the diffraction efficiencies of the two sets of holograms. Due to the bidirectionality of the optical bus, it is impossible to get uniform intensity fan-outs for all the cases where the modulated optical signals are incident from different channels. So, the best way to overcome this least-power-limitation problem is to try to balance the output power from different channels. This can be achieved by optimizing the diffraction efficiencies of the holographic gratings.

In relation to our experimental device, we consider the following bidirectional optical bus with 9 boards on one side of the substrate (as in Fig. 1). In our analysis we will assume that the diffraction efficiencies of the first set of hologram are, η_1, η_2, ... and η_9, from left to right, respectively. Due to symmetric requirement for optimization, the diffraction efficiencies for the second hologram array are η_1, η_2, ... and η_9, from right to left. To provide the optimized power budget, we have to impose the following criteria: $\eta_1 = 1$ and $\eta_9 = 0$, i. e., there is only one hologram at the 1st channel and the 9th channel. If we denote P_{ij} to be the output power at the jth channel when light is incident from the ith channel, and the same holds for P'_{ij}, except that they have a reversed propagating direction. We thus have

$$P_{ij} = 0 \qquad \text{whenever } i = j, \tag{5}$$

$$P'_{i1} = P'_{i9} = 0 \qquad i = 1, \ldots, 9. \tag{6}$$

Based on the argument we made above, it's easy to write the expressions for P_{ij}'s and P'_{ij}'s as functions of η_1 , ... and η_9. Then, the optimization process is as following. The goal is to find an optimized distribution of diffraction efficiencies leading to a fan-out intensity distribution with a minimum power fluctuation and therefore an optimized power budget. For this purpose, we need to generate an objective function[14]. By optimizing the objective function, a well balanced fan-out distribution can be reached. For our problem, the minimum fluctuation nature requires us to establish an objective function of the form

$$E = E_1 + E_2 \tag{7}$$

where

$$E_1 = \sum_{i=1}^{M}\left[\sum_{\substack{j=1\\ j\neq i}}^{N} W_{1ij}\left(\frac{P_{ij}}{\overline{P}}-1\right)^2 + \sum_{j=2}^{N-1} W'_{1ij}\left(\frac{P'_{ij}}{\overline{P}}-1\right)^2\right]$$

$$\text{for } P_{ij} \text{ and } P'_{ij} \geq \overline{P}, \tag{8}$$

$$E_2 = \sum_{i=1}^{M}\left[\sum_{\substack{j=1\\ j\neq i}}^{N} W_{2ij}\left(\frac{\overline{P}}{P_{ij}}-1\right)^2 + \sum_{j=2}^{N-1} W'_{2ij}\left(\frac{\overline{P}}{P'_{ij}}-1\right)^2\right]$$

$$\text{for } P_{ij} \text{ and } P'_{ij} < \overline{P}, \tag{9}$$

in which $\overline{P}$ is the average value of the fan-outs and, to effectively reduce the differences of each fan-outs from the average, we have added before each term the weight factors W_{1ij}, W'_{1ij}, W_{2ij} and W'_{2ij}, so that the fan-outs with bigger differences from $\overline{P}$ will be effectively dragged back. In our calculation, we used two different weights, one has an exponential form, the other has a non-exponential power form, and the same results has been obtained. A detailed discussion of our calculation will be presented in a future publication. Here, we provide the calculation results. Minimization of the objective function E eventually gives an optimized diffraction efficiency distribution

$$(\eta_1, \eta_2, \ldots, \eta_9) = (1.0,\ 0.3341,\ 0.2005,\ 0.1435,\ 0.1548,\ 0.1665,\ 0.2492,\ 0.4984,\ 0.0) \tag{10}$$

The resultant fan-out power distribution is summarized in Table 2.

For our backplane bus proposed in this paper, the sensitivity of a photodiode detector is a function of the input signal modulation speed, the bit error rate and the wavelength of the signal carrier. For a PIN-FET photodiode with a quantum efficiency of 50% at 1.3 μm, if the data transfer rate is 1.2 Gbit/sec, and the required error probability after amplification of the detector signal is less than 10^{-9}, then the minimum modulated power required at the detector site is determined to be 5.08×10^{-5} W. From Table 3, we see the ratio between the maximum and the minimum fan-out powers is about 47. This implies that the maximum power the detector should be able to handle before it saturates is around 2.39×10^{-3} W. The dynamic range of the detector can be employed to closely approximate the dynamic range of the receiver subsystem that will perform efficiently in conjunction with the optical backplane bus.

Theoretical Power Distribution

Output / Input	1	2	3	4	5	6	7	8	9
1	0	0.498	0.083	0.033	0.022	0.015	0.015	0.015	0.015
2	0.498	0	0.083	0.033	0.022	0.015	0.015	0.015	0.015
3	0.083	0.083	0	0.033	0.022	0.015	0.015	0.015	0.015
4	0.033	0.033	0.033	0	0.022	0.015	0.015	0.015	0.015
5	0.022	0.022	0.022	0.022	0	0.022	0.022	0.022	0.022

Table 2. Summary of the fan-out distribution obtained from theoretical analysis (not including P'_{ij} portion).

A bidirectional backplane bus with optimized power distribution and thus hologram diffraction efficiency, is provided for the demonstrated system, presented in Section 3. Discrepancy between experimental and theoretical results is observed. An optimized system shall provide us with a diffraction efficiency equivalent to the theoretical value, for each holographic element involved. Such an arrangement can be made by individually recording each hologram along a backplane bus.

6. System-related issues of optical backplane

In this section we address several issues related to the commercial viability of the bidirectional optical backplane. Precise alignment of optoelectronic components is vital to the reliable operation of optical backplane, especially, to support the electrical standard board separation of 3 cm. Since the thickness of the waveguiding plate should be increased, more strict restrictions on alignment must be made. Existing 2-D planar alignment techniques, which are developed for fabricating silicon VLSI circuits, can be employed to provide such a high precision needed to build the bi-directional optical backplane[15]. The laser diodes and the photodetectors can be flip-chip bonded to the glass substrate with the holograms recorded on it. They can be aligned to the substrate by means of alignment references that can be photolithographically transferred to the optical backplane bus[16].

Our bi-directional optical backplane can be easily expanded to implement multi-channel data paths by utilizing arrays of transceivers. There have been several different approaches[17][18] to utilize array devices. However, a number of recent attempts are stimulated by the advances of Vertical Cavity Surface Emitting

Lasers(VCSELs), which have evolved into efficient and reliable devices. VCSEL has many advantageous features for optical interconnection[19]. Some of those are small device size, low threshold current, small divergence angle, single longitudinal mode, and circular symmetric emission pattern. Yet another attractive feature of VCSEL technology is the capability of fabricating uniform, individually addressable, one and two dimensional arrays[20][21]. Many optical interconnection systems taking advantage of these VCSEL arrays have been developed or being manufactured[19][20][22]. Design issues using VCSEL arrays in free-space optical interconnects were addressed in the previous publication[23].

Crosstalk analysis is critical in devices where channels are designed by multiple exposures on the same emulsion area. The recording angle and the diffraction angle are different for each exposure. These parameters are changed to fabricate holograms with different grating periods. A fine example for such a device is a wavelength division demultiplexer (WDDM). Here the idea is to disperse signals at selected wavelengths[24]. In this case there can exist a state where there is optical signal in say, channel A while channel B is supposed to have no optical signal. But due to crosstalk, from channel A, some optical signal maybe detected in channel B.

In our device, even though the emulsion area is exposed twice, the recording parameters remain unchanged. So the periodicity of the gratings is the same. Crosstalk is not critical in our case since it is one optical signal that is guided in the substrate after it is coupled in by the input coupler and it is the same optical signal that is coupled out by the other diffraction holograms. A situation never arises where there is no optical signal in a channel at a particular time. In fact cross-coupling is an essential part of device operation. A theoretical treatment of the optimum energy distribution across the device, has already been presented in a preceding section. The system however can have a degradation of the signal-to-noise ratio due to crosstalk between the optoelectronic components involved, but this is a limitation associated with any communication system that incorporates optoelectronic devices at the source and detector end of each transceiver.

There are other factors that contribute to losses in the system that incorporates the optical backplane bus. There is a significant coupling loss associated with the optical bus. Only 20% of the input signal is coupled into the substrate. Reflection from the surface and transmission through the substrate contribute to this reduced coupling efficiency. However the coupled signal is sufficient for the efficient operation of any transceiver system, where the optical bidirectional backplane bus acts as the interconnect medium. There is also a 0.1 dB/cm propagation loss in the device, which translates to 0.6 dB in our device which is 6 cm long. The propagation loss is well within limits that are acceptable for existing commercial applications

As mentioned in Section 5, due to the characteristics of bus protocol and optical fan-out, there are inevitable fluctuations on the received power. Recent development of several burst-mode compatible optical receivers with wide dynamic range[25][26] can be utilized in future implementation of viable bidirectional optical backplane.

7. Conclusions

We have described the bidirectional optical backplane, operating at 632.8 nm and 1300 nm, and discussed its application to a high-performance backplane bus for multiprocessor systems. This is the first general purpose, bidirectional optical backplane bus aimed at multiprocessor systems. The reported optical backplane consists of multiplexed holograms in conjunction with a waveguiding plate with cascaded fan-out capability. A bidirectional optical backplane with nine boards is demonstrated. Data transfer rate of 1.2 Gbit/sec at the wavelength of 1300 nm is illustrated with a single bus line. Packaging-related issues, such as misalignment of transmitters and detector size limitation are further addressed, in order to provide a reliable system. A theoretical analysis aimed at minimizing intensity fluctuations among received powers has also been presented.

The bidirectional optical backplane reported herein, is transparent to all the higher layers of electrical bus protocol and can support all kinds of buses of interest, especially high performance multiprocessor buses, like Futurebus+, Multibus II, etc., as long as the appropriate protocols governing the rules of data transaction are provided. All the existing protocols for electrical buses can still be used for the optical backplane reported herein.

References

[1] P. Sweazey, "Limits of performance of backplane buses," in *Digital Bus Handbook*, edited by J. De Giacomo, McGraw-Hill, New York, 1990.

[2] IEEE Futurebus$^+$ P869.1: Logical Layer Specifications, Published by IEEE, New York, 1990.

[3] Ray T. Chen, "VME optical backplane bus for high performance computer," reprinted from *Optoelectronics-Device and Technologies*, 1994.

[4] J. W. Goodman, F. I. Leonberger, S.-Y. Kung, and R. A. Athale, "Optical interconnections for VLSI systems,"*Proc. IEEE* 72(7), pp. 850-866, 1984.

[5] J. P. G. Bristow, "Recent progress in optical backplane," presented at OE/LASE '94, Los Angeles, California 22-29 January 1994.

[6] J. Hyde, "The Multibus II bus structure," in *Digital Bus Handbook*, edited by J. De Giacomo, McGraw-Hill, New York, 1990.

[7] J. Yeh, and R. K. Kostuk, "Design issues for substrate mode holograms used in optical interconnects," *Proc. SPIE*, vol. 2176, pp. 207-217, 1994.

[8] Hans Peter Herzig and Rene Dandliker, "Diffractive components: holographic optical elements," in *Perspectives*

for Parallel Optical Interconnects, edited by Ph. Lalanne and P. Chavel, Springer-Verlag, New York 1993.
[9] Ray. T. Chen, Maggie Lee, Srikanth Natarajan, Chuan Lin, Z. Z. Ho, and Dan Robinson, "Single-mode Nd^{3+}-doped graded-index polymer waveguide amplifier," *IEEE Photonics Technology Letters.*, **vol. 5, no. 11**, 1993.
[10] Ray. T. Chen, Hey Lu, Daniel Robinson, Michael Wang, Gajendra Savant, and Tomasz Jannson, "Guided-wave planar optical interconnects using highly multiplexed polymer waveguide holograms," *Journal of Lightwave Technology.*, **vol. 10, no. 7**, pp. 888-897, 1992.
[11] Eric Bradley, Paul K. T. Yu, and Alan R. Johnston, "System issues relating to laser diode requirements for VLSI holographic optical interconnects," *Optical Engineering* , **vol. 28, no. 3**, pp.201-210, 1989.
[12] Herwig Kogelnik, "Coupled wave theory for thick hologram gratings," *The Bell System Technical Journal.*, **vol. 58, no. 9**, pp. 2909-2947, 1969.
[13] T. J. Kim, E. W. Campbell, and R. K. Kostuk,"Determination of average refractive index of spin coated DCG films for HOE fabrication," *Proc. SPIE* **vol. 1914**, pp. 91-100, 1993.
[14] *Management Science: An Introduction to Quantitative Analysis for Management*, eds. W. E. Pinney and D. B. Mcwilliams, Harper and Row Publisher, New York, 1982.
[15] Suning Tang, R. T. Chen, Dave Gerold, M. M. Li, Srikanth Natarajan, Jielun Lin, N. Chellappan and M. Peskin, "Design considerations for high packaging density optical bus array," *Proc. SPIE*, **vol. 2153**, pp. 227-235, 1994.
[16] Susant K. Patra, Jian Ma, Volkan H. Ozguz and Sing H. Lee, "Alignment issues in packaging for free-space optical interconnects," *Optical Engineering.*, **vol. 33, no. 5**, pp. 1561-1570, May 1994.
[17] A. Takai, T. Kato, S. Yamashita, S. Hanatani, Y. Motegi, K. Ito, H. Abe, and H. Kodera, "200-Mb/s/ch 100-m optical subsystem interconnections using 8-channel 1.3-mm laser diode arrays and single-mode fiber arrays," *Journal of Lightwave Technology* , **vol.12**, pp.260-269, 1994.
[18] T. Nagahori, M. Itoh, I. Watanabe, J. Hayashi, and H. Honmou, "150 Mbit/s/ch 12-channel optical parallel interface using an LED and a PD array," *Optics and Quantum Electronics* , **vol.24**, pp.S479-S489, 1992.
[19] R. A. Morgan, "Advances in Vertical Cavity Surface Emitting Lasers," *Proc. SPIE* , **vol.2147**, pp.97-119, 1994.
[20] D. Vakhshoori, J. D. Wynn, and G. J. Zydzik, "8 x 18 top emitting independently addressable surface emitting laser arrays with uniform threshold current and low threshold voltage," *Applied Physics Letters.*, **vol.62**, pp.1718-1720, 1993.
[21] A. von Lehmen, C. Chang-Hasnain, J. Wullert, L. Carrion, N. Stoffel, L. Florez, and J. Harbison, "Independently addressable InGaAs/GaAs Vertical cavity surface emitting laser arrays," *Electronics Letters* , **vol.27**, pp.583-585, 1991.
[22] R. A. Novotny, "Parallel optical data links using VCSELs," *Proc. SPIE* , **vol.2147**, pp.140-149, 1994.
[23] S. Tang, R. T. Chen, D. Gerald, M. M. Li, C. Zhao, S. Natarajan, and J. Lin, "Design limitations of highly parallel free-space optical
interconnects based on arrays of vertical-cavity surface emitting laser diodes, microlenses, and photodetectors," *Proc. SPIE* , **vol. 2153**, pp. 323-33, 1994.
[24] Ray T. Chen and H. Lu, "Polymer-based 12-channel single-mode wavelength division multiplexer on GaAs substrates," *Proc. SPIE*, **vol. 179**, pp 44, 1992.
[25] Y. Ota, and R. G. Swartz, "Burst-mode compatible optical receiver with a large dynamic range," *Journal of Lightwave Technology* , **vol. 8, no. 12**, pp. 1897-1902, 1990.
[26] Y. Ota and R. G. Swartz, "DC-1Gb/s burst-mode compatible receiver for optical bus applications," *Journal of Lightwave Technology* , **vol. 10, no. 2**, 244-249, 1992.